JOURNAL OF MATERIALS SCIENCE 24 (1989) 1109–1116

Work of adhesion and contact-angle isotherm of binary alloys on ionocovalent oxides

J. G. LI, L. COUDURIER, N. EUSTATHOPOULOS
Laboratoire de Thermodynamique et Physico-Chimie Métallurgiques, UA 29 CNRS, ENSEEG, BP 75, 38402 Saint Martin D'Heres Cédex, France

Using the monolayer approximation for metal–vapour and metal–oxide interfaces and Bragg–Williams statistics, a simple thermodynamic model has been constructed to calculate the variation in contact angle and work of adhesion as a function of composition in binary alloy–ionocovalent oxide systems. This model has been used to classify the curves of contact angle and the work of adhesion as a function of composition into three main types of isotherm. Model predictions and experimental results are compared using data on binary alloy–monocrystalline alumina systems.

1. Introduction

The energetic properties of liquid metal–ionocovalent oxide interfaces are usually described by two quantities:

(i) The contact angle, θ, of the liquid (L) on a solid (S) in vapour (V), related with the σ_{ij} interfacial tensions by Young's equation:

$$\cos\theta = \frac{\sigma_{SV} - \sigma_{SL}}{\sigma_{LV}} \quad (1)$$

(ii) The work of adhesion, W, defined by Dupre's equation:

$$W = \sigma_{SV} + \sigma_{LV} - \sigma_{SL} \quad (2)$$

and related to the contact angle by the equation

$$\cos\theta = \frac{W}{\sigma_{LV}} - 1 \quad (3)$$

Pure liquid metal (Me)–ionocovalent oxide (MO_n) systems can be classified in two categories [1] depending on the sign of the standard Gibbs free energy ΔG^0_R, of the reaction

$$n\mathrm{Me} + m\mathrm{MO}_n = n\mathrm{MeO}_m + m\mathrm{M} \quad (4)$$

In reactive systems, with a negative value of ΔG^0_R, wetting of the liquid on the ceramic occurs simultaneously with the formation of a new solid phase at the interface, and contact angles much smaller than 90° can then be obtained. An increase in temperature may lead to a considerable decrease in the value of θ ($-\mathrm{d}\theta/\mathrm{d}T$ may be as high as 0.2 deg K^{-1}) [1, 2]. For this class of systems Aksay *et al.* [3] and Naidich [1] have pointed out that the Gibbs free energy of reaction (Equation 4) makes an important contribution to the spreading driving force, while Standing and Nicholas [2] have suggested that the detailed chemistry and structure of the reaction products would also have a marked influence on wetting behaviour.

This work is devoted to the study of non-reactive metal–ionocovalent (refractory) oxide systems, that is systems with a positive value of ΔG^0_R. In truth, even in this case, some dissolution of the oxide into the metallic phase always occurs, but to a very small extent (a few p.p.m. or tens of p.p.m., depending on temperature, the nature of the liquid metal and the oxide, and the oxygen partial pressure in the vapour) and will thus be ignored. Typical values of contact angles of pure metals on refractory oxides (Al_2O_3, SiO_2, ZrO_2, MgO, etc.) lie between 80 and 145° [1, 4–6]. Corresponding values of the work of adhesion lie between 200 and 1200 mJ m^{-2} (Table I). The temperature coefficient of the contact angle is negative, but an order of magnitude lower, in absolute values, than that of reactive systems [7]. The temperature coefficient of the work of adhesion is positive but very small (from 0.05 to 0.5 mJ m^{-2} K^{-1} [7]).

From both thermodynamic model [6, 8] and electronic structure calculations [9, 10], it has been concluded that the interfacial bond in this kind of system is essentially chemical, resulting from weak electron transfers between the phases in contact.

The aim of this work is to predict the form of the contact angle and work of adhesion isotherms $\theta(x_B)$ and $W(x_B)$, respectively, of a non-reactive binary (A, B) alloy–ionocovalent oxide system from the known values of contact angle θ^A, θ^B and of work of adhesion W^A, W^B, of the corresponding pure metals. For this purpose, the slopes of these two quantities will be calculated at the two ends of the binary diagrams, i.e. at $x_B \to 0$ and $x_B \to 1$. Ignoring any variation in oxide surface tension with alloy composition, this is equivalent, according to Equations 1 and 2, to calculating the corresponding slope values of the $\sigma_{LV}(x_B)$ and $\sigma_{SL}(x_B)$ curves.

It should be noted that the assumption σ_{SV} = constant at a given temperature, which is reasonable for high contact angle systems, has recently been confirmed by Nikolopoulos [11] for metal–alumina systems. Using the "multiphase equilibrium" method, this author measured the surface tension of alumina

0022–2461/89 $03.00 + .12

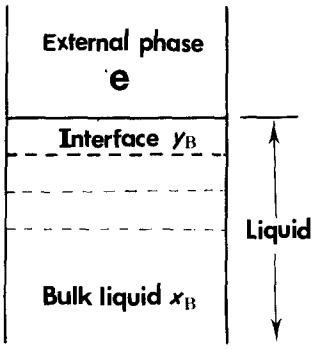

Figure 1 The monolayer model of a binary liquid–external phase interface.

under a neutral gas (argon) and a gas containing metallic vapour (tin or cobalt), and found that there was no difference in σ_{SV} values (Table II). Clearly, the adsorption of metallic atoms on ceramic surfaces is negligible in non-wetting systems.

2. Surface tension and interfacial tension calculations

2.1. Interface model and statistics

The system studied (Fig. 1) consists of a liquid phase (bulk liquid and interface) in contact with an external phase which will be given the index e. This external phase may be either a vapour phase or a solid of negligible solubility in the liquid alloy. The calculations are based on the following hypothesis:

1. The interface is limited to a monoatomic layer of N' atoms including $N'_A = N'y_A$ atoms of A and $N'_B = N'y_B$ atoms of B.
2. The N atoms of the liquid (comprising $N_A = Nx_A$ atoms of A and $N_B = Nx_B$ atoms of B) and the N' atoms of the interface are located on the sites of the same atomic lattice.
3. Only the interactions between an atom and its closest neighbours are taken into account.
4. It will be considered that the atomic distribution in the bulk liquid and in the interface is completely random (Bragg–Williams approximation).

The surface tension σ due to the presence of an interface of total area Ω (where $\Omega = N'\omega$, ω being the average area of a metallic atom at the interface) will be given by [12]

$$\sigma\Omega = F - \sum_{i=A,B} (N_i + N'_i)\mu_i \qquad (5)$$

where F is the free energy of the liquid (bulk liquid plus interface) and μ_i is the chemical potential of the species i in the bulk liquid. The total free energy F of the liquid will be calculated from the partition function Φ:

$$F = -kT \ln \Phi \qquad (6)$$

where k is Boltzmann's constant and T the temperature.

In a closed system, Φ takes the following form:

$$\Phi = \sum_{conf.} \exp\left(-\frac{E}{kT}\right) \qquad (7)$$

where E is the energy of a particular configuration, the sum being extended to all possible configurations. In the Bragg–Williams approximation, Φ is written

$$\Phi = \frac{N!}{N_A!N_B!}\frac{N'!}{N'_A!N'_B!}\exp\left(-\frac{\bar{E}}{kT}\right) \qquad (8)$$

$\bar{E}$ is the energy of the mean configuration corresponding to a completely random distribution of the atoms in both the bulk liquid and the interface. The free energy F is then written

$$F = kT(N_A \ln x_A + N_B \ln x_B + N'_A \ln y_A + N'_B \ln y_B) + \bar{E} \qquad (9)$$

The energy $\bar{E}$ can be calculated by summing all pair energy values. This is written as follows:

$$\begin{aligned}\bar{E} = {} & \left(\frac{zlN}{2} + zmN - \frac{zmN'}{2}\right) \\ & \times (x_A^2\varepsilon_{AA} + x_B^2\varepsilon_{BB} + 2x_Ax_B\varepsilon_{AB}) \\ & + \frac{zlN'}{2}(y_A^2\varepsilon_{AA} + y_B^2\varepsilon_{BB} + 2y_Ay_B\varepsilon_{AB}) \\ & + zmN'[y_Ax_A\varepsilon_{AA} + y_Bx_B\varepsilon_{BB} \\ & + (y_Ax_B + y_Bx_A)\varepsilon_{AB}] \\ & + zmN'(y_A\varepsilon_{A-e} + y_B\varepsilon_{B-e}) \end{aligned} \qquad (10)$$

where z is the coordination number in the liquid, l and m are the fractions of the nearest neighbours located respectively in the same layer and in an adjacent one ($l + 2m = 1$). ε_{ij} is the interaction energy of an ij pair in the liquid phase and ε_{i-e} the energy of a bond formed between the atom i and the external phase.

The chemical potential μ_i will be calculated by the relation

$$\mu_i = \left(\frac{\partial F}{\partial N_i}\right)_{T,V,N_{j\neq i}} \qquad (11)$$

TABLE I Values of surface tension σ_{LV}, contact angle θ and work of adhesion W, for a number of pure metals on monocrystalline alumina (after Chatain *et al.* [6])

Me	T (K)	σ_{LV} (mJ m^{-2})	θ (deg)	W (mJ m^{-2})
Ag	1373	905	130	323
Al	1150	834	82	950
Au	1373	1131	139	277
Cu	1423	1274	131	438
Ni	1730	1780	112	1113
Pb	1173	392	117	214
Si	1723	745	80	875
Sn	1373	478	123	218

TABLE II Influence of metallic vapours on the surface tension σ_{SV}, of alumina (after Nikolopoulos [11])

T (K)	Vapour	σ_{SV} (J m^{-2})
1473	Ar	1.41 ± 0.20
	Ar + Sn	1.44 ± 0.21
1623	Ar	1.28 ± 0.15
	Ar + Sn	1.31 ± 0.15
1783	Ar	1.19 ± 0.04
	Ar + Co	1.14 ± 0.04
1923	Ar	1.06 ± 0.06
	Ar + Co	1.02 ± 0.06

From Equations 9 and 10, neglecting the N'/N terms, the classic expression of the chemical potential of the element i is obtained in a regular binary solution:

$$\mu_i = \frac{z\mathcal{N}}{2}\varepsilon_{ii} + (1 - x_i)^2\lambda + RT \ln x_i \quad (12)$$

where λ is the molar exchange energy of the liquid AB alloy ($\lambda = z\mathcal{N}[\varepsilon_{AB} - (\varepsilon_{AA} + \varepsilon_{BB})/2]$) and $\mathcal{N}$ is Avogradro's number.

Considering Equations 5, 9, 10 and 12, the general equation for σ is obtained:

$$\begin{aligned}\sigma\Omega_M = {} & zm\mathcal{N}(y_A\varepsilon_{A\text{-}e} + y_B\varepsilon_{B\text{-}e}) \\ & - \frac{zm\mathcal{N}}{2}(y_A\varepsilon_{AA} + y_B\varepsilon_{BB}) \\ & + RT[y_A \ln(y_A/x_A) + y_B \ln(y_B/x_B)] \\ & + (l + m)\,x_Ax_B\lambda + ly_Ay_B\lambda \\ & - (l + m)(y_Ax_B + y_Bx_A)\lambda \quad (13)\end{aligned}$$

where Ω_M is the molar interfacial area ($\Omega_M = \mathcal{N}\omega$).

2.2. Expressions of surface tension and interfacial tension

By applying Equation 13 to the pure metal i (with i = A or B), the following relation is obtained:

$$\sigma^i\Omega^i_M = zm\mathcal{N}\varepsilon_{i\text{-}e} - \frac{zm\mathcal{N}}{2}\varepsilon_{ii} \quad (14)$$

Two cases are considered, depending on whether the external phase is the vapour (L–V surface) or the solid oxide (S–L interface).

2.2.1. Surface tension σ_{LV}

In this case, the relation $\varepsilon_{i\text{-}e} = \varepsilon_{i\text{-}V} = 0$ applies, and from Equations 13 and 14, the classic expressions for the surface tension of a pure metal, σ^i_{LV} and that of a regular binary alloy, σ_{LV}, are found [12]:

$$\sigma^i_{LV}\Omega^i_M = -\frac{zm\mathcal{N}}{2}\varepsilon_{ii} \quad (15)$$

and

$$\begin{aligned}\sigma_{LV}\Omega_M = {} & (y_A\sigma^A_{LV} + y_B\sigma^B_{LV})\Omega_M \\ & + RT[y_A \ln(y_A/x_A) + y_B \ln(y_B/x_B)] \\ & + (l + m)x_Ax_B\lambda + ly_Ay_B\lambda \\ & - (l + m)(y_Ax_B + y_Bx_A)\lambda \quad (16)\end{aligned}$$

For a given composition, x_B, of the bulk phase, the molar fraction y_B at the L–V surface is obtained by minimizing the free energy F (Equation 5) with respect to y_B, or what comes to the same thing, by minimizing $\sigma_{LV}\Omega_M$ with respect to y_B. The following equation is obtained:

$$\begin{aligned}RT \ln\left(\frac{y_B(1 - x_B)}{x_B(1 - y_B)}\right) & \\ = (\sigma^A_{LV} - \sigma^B_{LV})\Omega_M - l(1 - 2y_B)\lambda & \\ + (l + m)(1 - 2x_B)\lambda & \quad (17)\end{aligned}$$

The monolayer surface model of regular solutions (Equations 16 and 17) has been widely used to predict the surface tension of binary solutions [12, 13]. This model can describe the surface tension quantitatively for alloys having weak or moderate hetero-atomic interactions. When the λ/RT values are very positive (segregation in liquid phase), or very negative (clustering), the agreement between calculated and experimental values is much less satisfactory (for example, see in Fig. 2 the calculated and experimental results for the Cu–Sn system for which $\lambda/RT = -1.24$). For these types of system, the model correctly predicts the sign but only the order of magnitude of the surface tension slopes $d\sigma_{LV}/dx_B$ for $x_B \to 0$ and $x_B \to 1$. It is for this reason that this study is limited to the signs of variations in surface tension and interfacial tension at the limits $x_B \to 0$ and $x_B \to 1$. For this purpose, the coefficient of enrichment of Metal B at the surface is calculated from Equation 17:

$$\left(\frac{y_B}{x_B}\right)^{LV}_{x_B \to 0} = \exp\left(-\frac{E_{LV}(B)_A}{RT}\right) \quad (18)$$

where $E_{LV}(B)_A$ is the energy of adsorption of Element B at the surface of the Metal A from AB alloy infinitely diluted in B. This energy is expressed as follows:

$$E_{LV}(B)_A = (\sigma^B_{LV} - \sigma^A_{LV})\Omega_M - m\lambda \quad (19)$$

The variation in surface tension σ_{LV} due to the addition of Metal B at infinite dilution in the Metal A matrix is obtained by differentiating Equation 16 with respect to x_B. Taking into account Equations 18 and 19, the following expression is obtained:

$$\left(\frac{d\sigma_{LV}}{dx_B}\right)_{x_B \to 0} = \frac{RT}{\Omega_M}\left[1 - \exp\left(-\frac{E_{LV}(B)_A}{RT}\right)\right] \quad (20)$$

2.2.2. Interfacial tension σ_{SL}.

If the external phase is the solid oxide, from Equations 14 and 15 we find

$$\sigma^i\Omega^i_M = zm\mathcal{N}\varepsilon_{i\text{-}S} + \sigma^i_{LV}\Omega^i_M \quad (21)$$

where $\varepsilon_{i\text{-}S}$ is the energy of a bond between a metal atom i and the oxide. The term $zm\mathcal{N}\varepsilon_{i\text{-}S}$ thus represents the

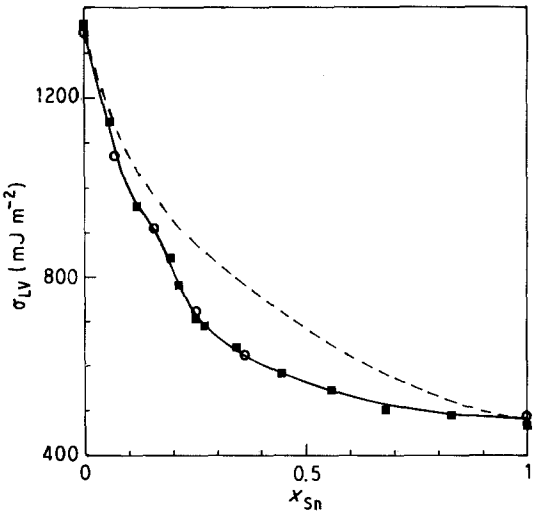

Figure 2 Comparison between experimental results from (○) Lauermann and Sauerwald [14] (■) Kwai *et al.* [15], and (– – –) results calculated with the monolayer model for the surface tension of the Cu–Sn system at 1423 K.

total bonding energy of one gram-atom of the metal i with the solid. Reduced to the unit interfacial area, this term is identical, with opposite sign, to the work of adhesion, W^i, of the metal i on the oxide:

$$-\frac{zm\mathcal{N}\varepsilon_{i\text{-}S}}{\Omega_M} = W^i \quad (22)$$

By including this expression in Equation 21 and comparing this with Equation 2, the following expression is obtained for the pure metal i:

$$\sigma^i = \sigma^i_{SL} - \sigma_{SV} \quad (23)$$

and for the alloy AB

$$\begin{aligned}(\sigma_{SL} - \sigma_{SV})\Omega_M &= [y_A(\sigma^A_{LV} - W^A) \\ &+ y_B(\sigma^B_{LV} - W^B)]\Omega_M \\ &+ RT[y_A \ln(y_A/x_A) + y_B \ln(y_B/x_B)] \\ &+ (l + m)\, x_A x_B \lambda + l y_A y_B \lambda \\ &- (l + m)(y_A x_B + y_B x_A)\lambda \end{aligned} \quad (24)$$

where y_B, the molar fraction of the metal B at the S–L interface, is the solution to the equation

$$\begin{aligned} RT \ln\left(\frac{y_B(1 - x_B)}{x_B(1 - y_B)}\right) \\ = (\sigma^A_{LV} - \sigma^B_{LV})\Omega_M - (W^A - W^B)\Omega_M \\ - l(1 - 2y_B)\lambda + (l + m)(1 - 2x_B)\lambda \end{aligned} \quad (25)$$

At limiting conditions, this equation reduces to

$$\left(\frac{y_B}{x_B}\right)^{SL}_{x_B \to 0} = \exp\left(-\frac{E_{SL}(B)_A}{RT}\right) \quad (26)$$

where $E_{SL}(B)_A$, the energy of adsorption of Metal B at the metal A–oxide interface from AB alloy infinitely diluted in B, can be expressed as follows:

$$\begin{aligned} E_{SL}(B)_A &= (\sigma^B_{LV} - \sigma^A_{LV})\Omega_M \\ &- (W^B - W^A)\Omega_M - m\lambda \end{aligned} \quad (27)$$

Assuming, as already mentioned, that the surface tension of the solid oxide is constant at a given temperature, this gives

$$\left(\frac{d\sigma_{SL}}{dx_B}\right)_{x_B \to 0} = \frac{RT}{\Omega_M}\left[1 - \exp\left(-\frac{E_{SL}(B)_A}{RT}\right)\right] \quad (28)$$

It should be noted that, according to Equation 2, $E_{SL}(B)_A$ can also be written as $E_{SL}(B)_A = (\sigma^B_{SL} - \sigma^A_{SL})\Omega_M - m\lambda$, which is similar to Equation 19 for $E_{LV}(B)_A$.

2.3. Evaluation of parameters

Equations 20 and 28 for the slopes of the $\sigma_{LV}(x_B)$ and $\sigma_{SL}(x_B)$ curves at the origin, include the following parameters:

(i) The energies of cohesion of the pure metals A and B, expressed in this model by the surface tension values of the pure metals, σ^A_{LV} and σ^B_{LV}. These quantities are known for a wide range of pure metals with an uncertainty factor of less than 5% [16].

(ii) The metal–solid bonding energies, expressed as the work of adhesion values of pure metals on the solid, W^A and W^B. For metal–alumina and metal–silica combinations, these values are known with sufficient accuracy (uncertainty factor less than 20%) for some fifteen different metals [6, 17]. For other combinations of Me–ionocovalent oxide MO_n, the values can be determined with an uncertainty factor of about 30% using the following expression, proposed by Chatain *et al.* [8]:

$$W_{Me\text{-}MO_n} = -\frac{\alpha}{\Omega_M}\left(\Delta\bar{H}_{(O)_{Me}} + \frac{1}{n}\Delta\bar{H}_{(M)_{Me}}\right) \quad (29)$$

where $\Delta\bar{H}_{(O)_{Me}}$ and $\Delta\bar{H}_{(M)_{Me}}$ are the enthalpies of mixing at infinite dilution of oxygen and oxide metal M in the liquid metal Me, and α is an empirical parameter equal to 0.20 [8].

(iii) The interaction energy between the metals A and B in the liquid alloy, expressed by the exchange energy of regular solutions, λ. This parameter is evaluated from the arithmetic mean of the tabulated values of partial mixing enthalpies of binary alloys AB at infinite dilution [18].

(iv) The molar volume values of the pure metals A and B, V^A_M and V^B_M, necessary for the calculation of the molar interfacial area, Ω^i_M, according to the following expression [13]:

$$\Omega^i_M = 1.091\mathcal{N}\left(\frac{V^i_M}{\mathcal{N}}\right)^{2/3} \quad (30)$$

For the alloy, the value $\Omega_M = (\Omega^A_M + \Omega^B_M)/2$ was taken.

(v) The structure parameter m, equal to 1/4 for liquid metals [13].

2.4. Properties of $\sigma_{LV}(x_B)$ and $\sigma_{SL}(x_B)$ isotherms

Details will now be given of some properties of surface and interfacial tension curves at $x_B \to 0$ and $x_B \to 1$. All these properties will be used to establish the contact angle and work of adhesion isotherms of a binary alloy on oxide.

(a) The first property, which is valid for any monolayer model of a surface or an interface, results directly from Equations 20 and 28. Following these equations for a binary system, if $E(B)_A/RT$ is very negative, the slope $(d\sigma/dx_B)_{x_B \to 0}$ will also be very negative. Conversely, if $E(B)_A/RT$ is very positive, this slope will be positive, but very small (Fig. 3a). The maximum value of $(d\sigma/dx_B)_{x_B \to 0}$ will in fact be equal to RT/Ω_M which, taking typical values of temperature (1000 K) and molar surface area (for example, $\Omega_M \simeq 5 \times 10^4\ m^2\ mol^{-1}$), gives the quite negligible value of $2\ mJ\ m^{-2}$ per 1% of solute. Note that this behaviour predicted by the monolayer model is well verified by the experimental surface tension values of binary alloys [19].

(b) The second property results from the fact that, in general, the absolute value of the interaction term in Equations 19 and 27, $|m\lambda|$, is much lower than that of the capillary terms, $|\sigma^B_{LV} - \sigma^A_{LV}|\Omega_M$ and $|W^B - W^A|\Omega_M$. Consequently, for both E_{LV} and E_{SL} energies of adsorption for a binary alloy, the following relation applies:

$$E(B)_A \ll 0 \rightleftharpoons E(A)_B \gg 0 \quad (31)$$

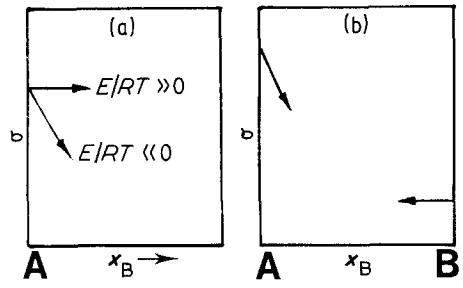

Figure 3 (a, b) Properties of $\sigma_{LV}(x_B)$ and $\sigma_{SL}(x_B)$ isotherms.

Thus, if the slope of the σ against x_B curve at $x_B \to 0$ is negative, the slope at $x_B \to 1$ will be nearly equal to zero (Fig. 3b, see also Fig. 2 for the surface tension of the Cu–Sn system).

(c) The third property is easily derived by comparing Equations 19 and 27 to obtain

$$E_{SL}(B)_A = E_{LV}(B)_A - (W^B - W^A)\Omega_M \quad (32)$$

According to this equation, the process of adsorption of a solute B from the bulk liquid at the Metal A–oxide interface can be broken down into two stages: in the first, the solute adsorbs at the liquid free surface; in the second, the solid approaches from an infinite distance, and makes contact with the liquid surface forming a solid–liquid interface.

Equation 32 explains why some authors have, in the past, postulated that a solute that is tensioactive at a liquid surface would also be tensioactive at the interface formed between the liquid and a solid. Evidently, this "intuitive idea" is correct only if the adhesion energy term is small compared to the surface tension term.

On the other hand, McDonald and Eberhart [20] suggested that the adsorption of Solute B at a liquid metal–solid oxide interface would be possible if the work of adhesion of the solute is greater than that of the matrix. This is true only if the surface tension term is small compared to the adhesion energy term. This is probably satisfied when, for example, both solute and matrix are ferrous metals, but not for any combinations of high and low melting point metals.

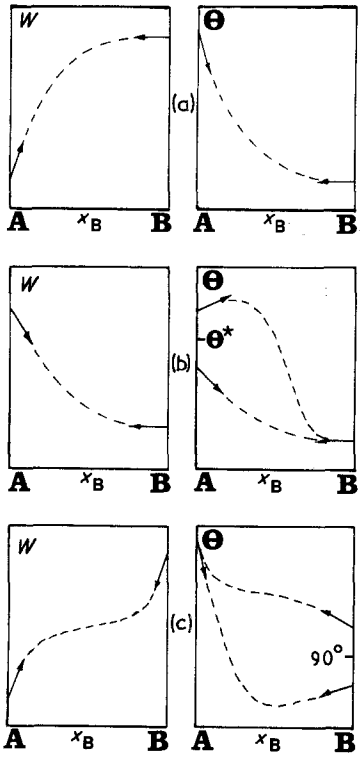

Figure 4 (a–c) Possible forms of the various types of $W(x_B)$ and $\theta(x_B)$ isotherms for AB–oxide systems.

3. Classification of $W(x_B)$ and $\theta(x_B)$ isotherms

From Equations 1 and 2, and taking into account Equations 20 and 28, the following relations are obtained:

$$\left(\frac{dW}{dx_B}\right)_{x_B\to 0} = \left(\frac{d\sigma_{LV}}{dx_B}\right)_{x_B\to 0} - \left(\frac{d\sigma_{SL}}{dx_B}\right)_{x_B\to 0}$$
$$= \frac{RT}{\Omega_M}\left[\exp\left(-\frac{E_{SL}(B)_A}{RT}\right) - \exp\left(-\frac{E_{LV}(B)_A}{RT}\right)\right] \quad (33)$$

and

$$\left(\frac{d(\cos\theta)}{dx_B}\right)_{x_B\to 0} = -\frac{1}{\sigma^A_{LV}}\left[\left(\frac{d\sigma_{SL}}{dx_B}\right)_{x_B\to 0} + \left(\frac{d\sigma_{LV}}{dx_B}\right)_{x_B\to 0}\cos\theta^A\right]$$
$$= -\frac{RT}{\sigma^A_{LV}\Omega_M}\left\{\left[1 - \exp\left(-\frac{E_{SL}(B)_A}{RT}\right)\right] + \left[1 - \exp\left(-\frac{E_{LV}(B)_A}{RT}\right)\right]\cos\theta^A\right\} \quad (34)$$

For AB–oxide systems, the model predicts three main types of $W(x_B)$ and $\theta(x_B)$ isotherms depending on the absolute and relative values of the adsorption energies $E_{LV}(B)_A$ and $E_{SL}(B)_A$. The forms of $W(x_B)$ and $\theta(x_B)$ isotherms corresponding to these three cases are examined below and a few examples are given for AB–monocrystalline alumina systems.

3.1. $E_{SL}(B)_A < E_{LV}(B)_A < 0$.

These inequalities valid for $x_B \to 0$, correspond to the $E_{SL}(A)_B > E_{LV}(A)_B > 0$ inequalities when $x_B \to 1$. This case occurs when $\sigma^B_{LV} < \sigma^A_{LV}$ and $W^B > W^A$. The element B is tensioactive both at the metal A surface and at the metal A–oxide interface, although more so at the interface than at the surface. As a result, the work of adhesion W increases (Equation 2) and the contact angle decreases (Equation 3) when small quantities of B are added to Metal A. On the other hand, addition of A to Metal B has virtually no effect on these parameters (Table III and Fig. 4a).

The (Cu–Al)–Al_2O_3 system corresponds to these cases, as indicated by the adsorption energy values given in Table IV. The experimental isotherms $W(x_{Al})$ and $\theta(x_{Al})$ are indicated in Fig. 5 [21]. It is worth noting that, following problems induced by aluminium oxidation [21], the contact angle isotherm at 1423 K in the copper-rich field could not be determined. This problem was overcome by increasing the temperature to 1523 K [21]. The experimental results

TABLE III Different possible types of work of adhesion and contact angle isotherms, depending on the values of adsorption energies at the liquid–vapour and liquid–solid oxide interfaces

Adsorption energies of Solute B in Matrix A	Conditions	$x_B \to 0$		$x_B \to 1$		Type	Examples (A–B)
		$\frac{dW}{dx_B}$	$\frac{d\theta}{dx_B}$	$\frac{dW}{dx_B}$	$\frac{d\theta}{dx_B}$		
$E_{SL} < E_{LV} < 0$	$\sigma_{LV}^B < \sigma_{LV}^A$ $W^B > W^A$	>0	<0	$\simeq 0$	$\simeq 0$	1	Cu–Al
$E_{LV} < E_{SL} < 0$	$\sigma_{LV}^B < \sigma_{LV}^A$		>0 if $\theta^A > \theta^{*\dagger}$			(2a)	Cu–Sn
	$W^B < W^A$	<0		$\simeq 0$	$\simeq 0$	2	
	$(\sigma_{LV}^B - \sigma_{LV}^A) < (W^B - W^A)$		<0 if $\theta^A < \theta^{*\dagger}$			(2b)	Ni–Cr
$E_{SL} < 0 < E_{LV}$	$\sigma_{LV}^B < \sigma_{LV}^A$				>0 if $\theta^B > 90°$	(3a)	(Sn–Ge)
	$W^B < W^A$	>0	<0	>0		3	
	$(\sigma_{LV}^B - \sigma_{LV}^A) < (W^B - W^A)$				>0 if $\theta^B < 90°$	(3b)	Sn–Al

$^\dagger \cos\theta^* \simeq -\exp[(W^B - W^A)\Omega_M/RT]$.

show that the contact angle decreases and work of adhesion increases when aluminium is added to copper. Conversely, small additions of copper to the aluminium do not cause any significant variations in contact angle or work of adhesion of the aluminium.

3.2. $E_{LV}(B)_A < E_{SL}(B)_A < 0$

These inequalities correspond to $E_{LV}(A)_B > E_{SL}(A)_B > 0$. This case occurs when $\sigma_{LV}^B < \sigma_{LV}^A$, $W^B < W^A$ and $(\sigma_{LV}^B - \sigma_{LV}^A) < (W^B - W^A)$. The element B is more tensioactive at the metal A surface than at the metal A–oxide interface. Consequently, the work of adhesion decreases (Equation 2) when Element B is added to Metal A. On the other hand, the addition of A to Metal B does not affect this parameter.

As far as the contact angle is concerned, the calculation shows that there is virtually no effect when A is added to Metal B. For an alloy diluted in B, the variation in θ depends not only on the adsorption energy values, but also on the contact angle θ^A of the A–oxide system with respect to a critical value, θ^*, defined (see Equation 34) by

$$\cos\theta^* = -\frac{1 - \exp[-E_{SL}(B)_A/RT]}{1 - \exp[-E_{LV}(B)_A/RT]} \simeq -\exp\left(\frac{(W^B - W^A)\Omega_M}{RT}\right) \quad (35)$$

When θ^A is lower than θ^*, adding B to Metal A leads to a decrease in contact angle. On the other hand, when θ^A is greater than θ^*, the contact angle increases (Table III and Fig. 4b).

Note that, in all cases, as the effects of Element B on the work of adhesion and on surface tension partly cancel each other out (Equation 3), the slopes at the origin $(d\theta/dx_B)_{x_B \to 0}$ will be small in absolute values.

The (Cu–Sn)–Al_2O_3 combination belongs to this type of system (Table IV). The experimental results at 1423 K (Fig. 6) [22], in agreement with model predictions, show that additions of copper in tin have practically no effect on the contact angle and work of adhesion of tin. Similarly, the model correctly predicts the experimentally observed decrease in the work of adhesion of copper as a function of x_{Sn}. On the other hand, the calculation predicts a slight increase in θ for copper when tin is added (thus, for this system $\theta^* \simeq 110° < \theta_{exp}^{Cu} \simeq 131°$), whereas the experimental results indicate a zero slope $(d\theta/dx_{Sn})$ for $0 < x_{Sn} < 0.20$. It is possible that the dispersion of experimental values of θ ($\pm 3°$) is too great to highlight the possible existence of a maximum contact angle in this system.

The (Ni–Cr)–Al_2O_3 combination, which also belongs to this type of system (Table IV), has been studied by several authors, but only for nickel-rich alloys. These studies show that additions of about 10 at % Cr in nickel lead to a 10 to 20° reduction in contact angle of this metal on alumina [23–25]. This result is in qualitative agreement with the model described here, which predicts that the slope $(d\theta/dx_{Cr})_{x_{Cr} \to 0}$ is negative since $\theta^* = 144° > \theta_{exp}^{Ni} \simeq 110°$.

TABLE IV Evaluation of $E_{LV}(B)_A$ and $E_{SL}(B)_A$ adsorption energy values in AB–Al_2O_3 systems

A–B	T (K)	λ [18] (kJ mol^{-1})	Ω_M [13] (10^4 m^2 mol^{-1})	$E_{LV}(B)_A$ (kJ mol^{-1})	$E_{SL}(B)_A$ (kJ mol^{-1})	Type
Cu–Al	1423	−26.9	4.2	−15.2	−41.4	1
Al–Cu				+28.7	+54.8	
Cu–Sn	1423	−14.7	5.1	−39.0	−27.7	2a
Sn–Cu				+46.3	+35.1	
Ni–Cr*	1773	−10.5	3.7	−7.7	−3.6	2b
Sn–Al	1273	+19.5	5.6	+14.0	−27.7	3b
Al–Sn				−23.7	+18.0	

* Using $W_{Cr} = 1000$ mJ m^{-2} estimated by Equation 29 and $\sigma_{LV}^{Cr} = 1500$ mJ m^{-2} [16].

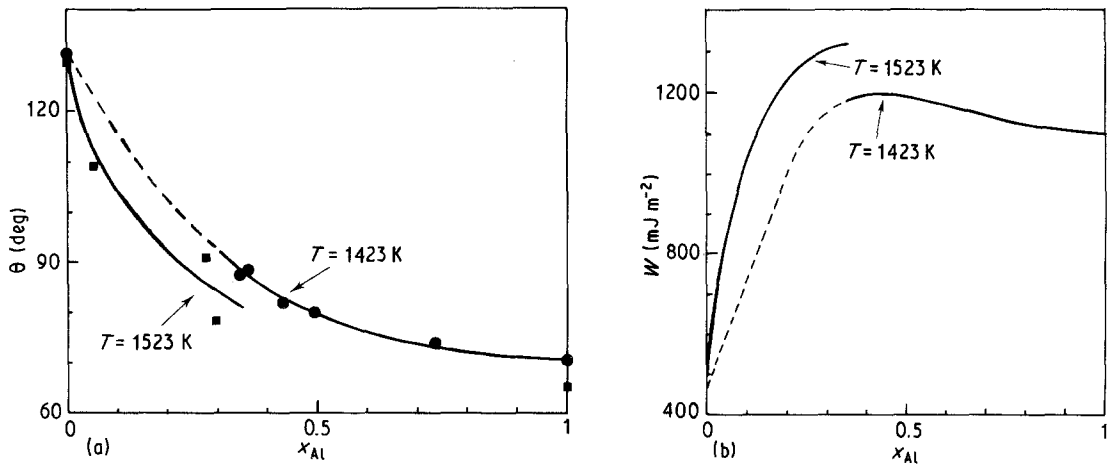

Figure 5 (a) Experimental contact angle and (b) work of adhesion isotherms of the (Cu–Al)–Al_2O_3 system [21].

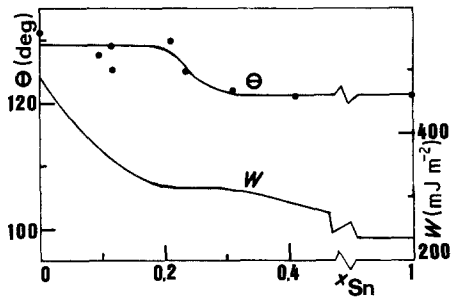

Figure 6 Experimental $\theta(x_{Sn})$ and $W(x_{Sn})$ isotherms for the (Cu–Sn)–Al_2O_3 system at 1423 K [22].

3.3. $E_{SL}(B)_A < 0 < E_{LV}(B)_A$

These inequalities correspond to $E_{SL}(A)_B > 0 > E_{LV}(A)_B$. This case occurs when $\sigma^B_{LV} > \sigma^A_{LV}$, $W^B > W^A$ and $(\sigma^B_{LV} - \sigma^A_{LV}) < (W^B - W^A)$. Element B is tensioactive at the metal–oxide interface, but is not at the Metal A surface. Consequently, the addition of B in Metal A causes an increase in the work of adhesion, and the addition of A in Metal B has the reverse effect (Table IV and Fig. 4c).

As far as the contact angle is concerned, the model predicts that it will decrease when Metal B is added to Metal A. For the reverse case (addition of A to B), two cases are possible depending on the value of contact angle, θ^B, of the B–oxide system:

(i) When θ^B is greater than 90°, the addition of A to Metal B leads to an increase in contact angle.

(ii) On the other hand, when θ^B is less than 90°, such an addition reduces the contact angle.

In the latter case, as θ decreases at the two ends of the binary diagram, the $\theta(x_B)$ curve has a minimum in the intermediate concentration field (Table III and Fig. 4c).

The (Sn–Al)–Al_2O_3 combination corresponds to this type of system (Table IV). The experimental isotherms $\theta(x_{Al})$ and $W(x_{Al})$ determined at 1273 K [26] are shown in Fig. 7. When aluminium is added to the Sn–Al_2O_3 system, the contact angle decreases and the work of adhesion increases due to the interfacial tension decreasing. The addition of tin to aluminium causes a reduction in work of adhesion and, as θ^{Al} is less than 90°, the contact angle decreases because the surface tension decreases. Thus, the experimental results show that the contact angle does effectively pass through a minimum value, as predicted by the model.

For systems of this type with $\theta^B > 90°$ (Type 3a in Table III), no examples were found in available literature. The model nevertheless predicts that such systems as Sn–Ge or In–Ge on alumina would belong to this type.

4. Conclusions

A simple model has been constructed, based on a monolayer surface and interface description and on

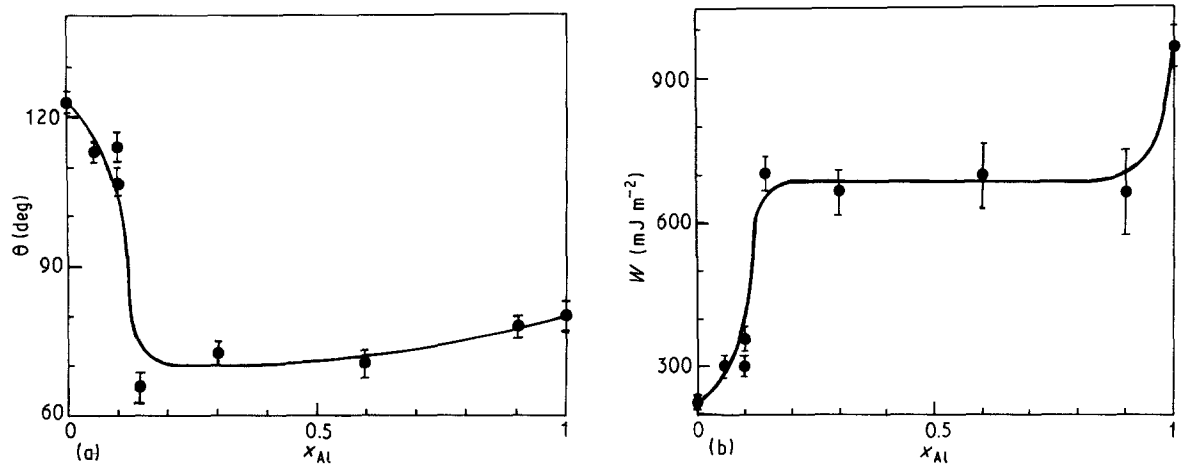

Figure 7 (a) Experimental contact angle and (b) work of adhesion isotherms for the (Sn–Al)–Al_2O_3 system at 1273 K [26].

Bragg–Williams statistics. This model has been used to calculate work of adhesion and contact angle isotherms of AB binary alloys on an ionocovalent oxide. The calculations need the knowledge of four types of parameter: surface tensions of the pure A and B metals, work of adhesion of Elements A and B on the oxide, exchange energy of the regular AB alloy, and molar volumes of the pure metals A and B. The model predicts three main types of $W(x_B)$ and $\theta(x_B)$ isotherms. Based on the experimental results obtained on AB–Al_2O_3 systems, it has been shown here that these predictions are indeed verified.

Using this model, it is also possible to propose thermodynamic criteria which enable B addition elements to be chosen with a view to obtaining both a reduction in contact angle and an increase in work of adhesion of a Metal A–oxide system. To this effect, the most favourable conditions are $\sigma^B_{LV} < \sigma^A_{LV}$ and $W^B > W^A$. When these conditions are satisfied, repulsive interactions ($\lambda > 0$) between A and B in the liquid alloy amplify the beneficial effect of Element B on W and θ; attracting interactions ($\lambda < 0$) attenuate this effect as they lead to a decrease in B solute activity in the alloy. In the latter case, it is possible to achieve an increase in B solute activity by introducing a third suitably-chosen metal in the AB alloy [22, 27].

Acknowledgement

This work was supported by the European Economic Community (Project No. ST2J-0150).

References

1. Ju. V. NAIDICH, *Progr. Surf. Membrane Sci.* **14** (1981) 353.
2. R. STANDING and M. NICHOLAS, *J. Mater. Sci.* **13** (1978) 1509.
3. I. A. AKSAY, C. E. HOGE and J. A. PASK, *J. Phys. Chem.* **78** (1974) 1178.
4. N. EUSTATHOPOULOS and A. PASSERONE, in Proceedings, 7èmes Journées Internationales Physico-Chimie et Sidérurgie, Versailles, 1978, p. 61.
5. D. BERUTO, L. BARCO and A. PASSERONE, in "Oxides and Oxide Films", edited by Ashok K. Vijh (Dekker, New York, 1981) p. 1.
6. D. CHATAIN, I. RIVOLLET and N. EUSTATHOPOULOS, *J. Chim. Physique* **83** (1986) 561.
7. I. RIVOLLET, D. CHATAIN and N. EUSTATHOPOULOS, *Acta Metall.* **35** (1987) 835.
8. D. CHATAIN, I. RIVOLLET and N. EUSTATHOPOULOS, *J. Chim. Physique* **84** (1987) 201.
9. K. H. JOHNSON and S. V. PEPPER, *J. Appl. Phys.* **53** (1982) 6634.
10. P. HICTER, D. CHATAIN, A. PASTUREL and N. EUSTATHOPOULOS, to be published.
11. P. NIKOLOPOULOS, *J. Mater. Sci.* **20** (1985) 3993.
12. R. DEFAY, I. PRIGOGINE, A. BELLEMANS and D. H. EVERETT, "Surface Tension and Adsorption" (Longmans, London, 1966) p. 160.
13. N. EUSTATHOPOULOS and J. C. JOUD, in "Current Topics in Materials Science", Vol. 4, edited by E. Kaldis (North-Holland, Amsterdam, 1980) p. 281.
14. V. I. LAUERMANN and F. SAUERWALD, *Z. Metallkde* **55** (1964) 605.
15. Y. KWAI, M. KISHIMOTO and T. TSUEN, *J. Jap. Inst. Met.* **37** (1973) 668.
16. L. D. LUCAS, "Techniques de l'Ingénieur" (Paris M67, 1984) p. 1.
17. R. SANGIORGI, M. L. MUOLO, D. CHATAIN and N. EUSTATHOPOULOS, *J. Amer. Ceram. Soc.*, in press.
18. R. HULTGREN, P. D. DESAI, D. T. HAWKINS, M. GLEISER and K. K. KELLY, "Selected Values of the Thermodynamic Properties of Binary Alloys" (American Society of Metals, Ohio, 1973).
19. M. BRUNET, J. C. JOUD, N. EUSTATHOPOULOS and P. DESRE, *J. Less-Common Metals* **51** (1977) 69.
20. J. E. McDONALD and J. G. EBERHART, *Trans. Met. Soc. AIME* **223** (1965) 512.
21. J. G. LI, L. COUDURIER and N. EUSTATHOPOULOS, *Rev. Int. Hautes Temper. Refract.* **24** (1988) 85.
22. J. G. LI, L. COUDURIER, I. ANSARA and N. EUSTATHOPOULOS, *Ann. Chim. Sci. Mat.* **13** (1988) 145.
23. W. M. ARMSTRONG, A. C. D. CHAKLADER and J. F. CLARKE, *J. Amer. Ceram. Soc.* **45** (1962) 115.
24. J. E. RITTER and M. S. BURTON, *Trans. Met. Soc. AIME* **239** (1967) 21.
25. R. M. CRISPIN and M. NICHOLAS, *J. Mater. Sci.* **11** (1976) 17.
26. J. G. LI, D. CHATAIN, L. COUDURIER and N. EUSTATHOPOULOS, *J. Mater. Sci. Letts.*, in press.
27. M. G. NICHOLAS, T. M. VALENTINE and M. J. WAITE, *J. Mater. Sci.* **15** (1980) 2197.

Received 4 January
and accepted 6 May 1988